A direct comparison of single-walled carbon nanotubes and quantum-wells based subpicosecond saturable absorbers for all optical signal regeneration at 1.55 μm

H. Nong,[a] M. Gicquel, L. Bramerie, M. Perrin, F. Grillot, C. Levallois, A. Maalouf, and S. Loualiche

Université Européenne de Bretagne, CNRS, Laboratoire Foton, INSA de Rennes, 20 Avenue des Buttes de Coësmes, 35708 Rennes, Cedex 7, France

(Received 27 November 2009; accepted 17 January 2010; published online 10 February 2010)

Subpicosecond optical transmission experiments are used to compare saturable absorber (SA) based on bundled single-walled carbon nanotubes (SWNT) and iron-doped InGaAs/InP epitaxial multiple quantum wells (MQW) at 1.55 μm telecom wavelength. The SA key parameters (contrast ratio, saturation fluence, and recovery time) relevant for high speed all optical signal regeneration (AOSR) are extracted from the normalized differential transmission (NDT). Although both SA exhibit good contrast ratios, SWNT show a full signal recovery as well as a much faster response time than MQW. This original work on SA shows that SWNT are excellent candidates for future low cost AOSR. © *2010 American Institute of Physics*. [doi:10.1063/1.3309712]

According to the development of ultra-high-bit-rate optical telecommunication systems, signal regeneration is required in order to improve signal-to-noise ratio, as telecom signal purity is degraded during its propagation along the fiber network. One possible solution which is relevant in the telecom wavelength range relies on the use of a saturable absorber (SA).[1] Actions of a SA result from its nonlinear absorption characteristics. The SA is an all-optical passive switch which acts either as an absorber when low incident light intensity is passed through it (SA blocking state) or as a transmitter under high incident light intensity (SA passing state). Three key-parameters of SA can be defined to ensure efficient light signal regeneration: an ultrafast optical switching speed between passing and blocking states, a high contrast ratio between both states as well as a low saturation fluence.

Prior work has already demonstrated SA based on multiple-quantum-wells (MQW) InGaAs/InP with improved switching time dynamics.[2] This result has been obtained by exploring excitonic optical properties of MQW with high concentration of iron atoms (Fe). Fe atoms which act as recombination centers for photo-generated carriers in such two-dimensional-nanomaterials enabled to decrease the MQW photoresponse time from nanosecond range to subpicosecond scale.[3]

Since their discovery in 1991,[4] single-walled carbon nanotubes (SWNT) are the subject of impressive number of research investigations. Their one-dimensional (1D) structure, which can be described as a rolled-up graphene sheet, leads to original electronic and associated optical properties.[5,6] Among them, previous pump-probe spectroscopy studies have revealed ultrafast carrier dynamics, especially in bundled SWNT.[7] Mode-locked lasers with SWNT based SA have also been demonstrated for short-pulses generation down to the subpicosecond scale within the near-infrared region.[8,9] These 1D-nanomaterials seem to have great potential for high quality subpicosecond all optical signal regeneration (AOSR).[10,11]

In this letter, in addition to previous works, we report a comparative study on well known MQW nanostructures, used as a reference based SA, with bundled SWNT for AOSR. We propose a direct comparison of SA efficiency based on MQW and on bundled SWNT using a cross-polarized pump-probe experiment, with femtosecond pulses in a degenerate configuration at 1.55 μm wavelength (minimum attenuation of light in telecom optical fiber). MQW-based SA were grown by gas-source molecular-beam epitaxy (MBE). They were made of 40 periods of InGaAs/InP MQW doped with Fe only in wells at 8.5×10^{18} cm^{-3}. Complex fabrication steps are involved in the process of ultrafast MQW-based SA in particular during their growth by MBE. The precise thickness value of MQW tunes their excitonic resonance peak to the desired 1.55 μm wavelength and the Fe doping concentration value controls the time constant of photogenerated carriers.[2] The transmission spectrum of Fe doped MQW is presented in Fig. 1(a). The excitonic resonance at 1.55 μm corresponds to a mixture of heavy and

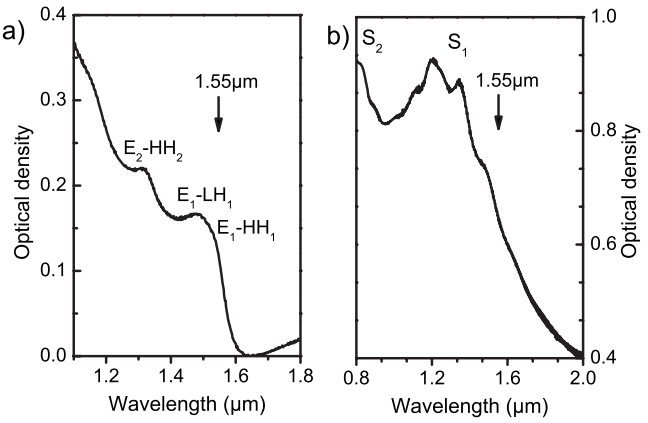

FIG. 1. (a) Optical transmission spectra of 40 MQW doped at 8.5×10^{18} cm^{-3} (only in wells), first excitonic resonances are mentioned. (b) Optical transmission spectra of bundled SWNT deposited on glass substrate, S_1 and S_2 denote first excitonic resonances of semiconducting SWNT.

[a]Author to whom correspondence should be addressed. Electronic mail: hanond.nong@insa-rennes.fr.

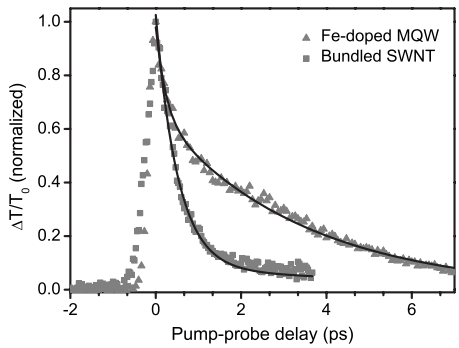

FIG. 2. Normalized NDT for Fe-doped MQW InGaAs/InP (triangle symbols) in direct comparison with bundled SWNT HiPCO (square symbols). Spectra were recorded in the same experimental run, namely same incident pump fluence and wavelength (40 μJ cm^{-2} and 1.55 μm respectively). Decay times are obtained by curve-fitting (continuous lines). The saturation absorption dynamics is described by a biexponentional for MQW (τ_x =0.23 ps and $\tau_{e/h}$=3.42 ps) and by a monoexponential for bundled SWNT (τ=0.51 ps).

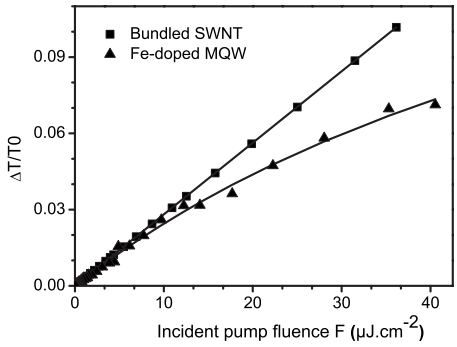

FIG. 3. NDT for Fe-doped MQW and bundled SWNT as a function of input pump fluence at excitation wavelength of 1.55 μm. Using the saturation law, values of FS are extracted from the curve-fitting at a null pump-probe delay (continuous lines): 70 μJ cm^{-2} with A=0.19, and 726 μJ cm^{-2} with A=2.04 respectively for MQW and bundled SWN.

light hole transitions, as these optical transitions are broadened because of the high Fe doping. The decrease in decay time is attributed to the relaxation mechanism between neutral Fe state in its Fe^{3+} configuration in wells with photogenerated electrons and holes.[12,13]

SWNT used in this work were grown using a modified gas phase process (HiPCO), and were supplied by Carbon Nanotechnologies Inc. The raw material was initially dispersed and sonicated in N-methyl pyrrolidone. The sample consisted of SWNT deposited on glass substrate from nitrogen-brushed SWNT dispersion. As a first comparison, Fig. 1(b) shows a transmission spectrum of bundled SWNT. The absorption band of interest near 1.55 μm corresponds here to the inhomogeneous broadened first optical transition of semiconducting nanotubes (S_1). Transitions in SWNT possess strong bound excitonic behavior in respect with interband electronic transitions described as S_i, where index i accounts for valence and conduction subbands of the SWNT Van Hove singularities.[14,15] These experimental data of bundled SWNT linear absorption suggest that a population of SWNT can be excited at 1.55 μm in order to achieve transient photobleaching of their optical excitonic transitions.

In order to demonstrate the ultrafast optical switching properties of these nanomaterials, pump-probe experiments were performed to determine precisely the nonlinear absorption dynamics at 1.55 μm in a transmission configuration. The optical excitation pulses (0.13 ps duration, 82 MHz repetition rate, and 1.3–1.6 μm wavelength range) originate from an optical parametric oscillator (OPO) source pumped by a Ti:sapphire femtosecond laser beam at 0.81 μm. The pump and the probe pulses are obtained by splitting off a part of the output beam. Then the probe beam is attenuated by a factor of 10^3 in order to prevent probe-induced nonlinearities. Both beams, with spot diameter of 60 μm, were focused onto the sample. A chopper is used to modulate pump beam intensity and the probe beam is detected through a lock-in amplifier. The normalized differential transmission (NDT) [$\Delta T/T_0$, where $\Delta T=T-T_0$ and $T_0(T)$ is the transmission of the probe at very low (high) pump excitation fluence] was recorded as a function of the time delay between the probe and the pump pulses. The experimental results, measured in a same experimental run, are presented in Fig. 2, which shows a direct comparison between the normalized NDT of MQW and the one of bundled SWNT at room temperature.

The maximum of the probe transmission is assigned to the photobleaching of the absorption band at 1.55 μm corresponding to a maximum number of photogenerated and probed excitons, by pump and probe pulses, respectively. From the transient dynamics observed in this degenerate configuration, it is obvious that photoexcitons optically created in SWNT decay much faster than in MQW sample. Data obtained for MQW can be curve-fitted by a biexponential indicating two decay time constants of 0.23 and 3.42 ps. The first time constant corresponds to the excitons dissociation time (τ_x), as excitonic binding energy in MQW is lower than thermal energy at room temperature [~5 meV for InGaAs MQW lattice matched on InP (Ref. 16)]. This excitonic dissociation is followed by free carriers capture through Fe atom traps introduced by Fe doping in MQW and corresponds to the second decay time[2] ($\tau_{e/h}$). On the other hand, the temporal response of SWNT perfectly fits a monoexponential behavior with a decay time constant of 0.51 ps (τ).

This direct comparison indicates that excitonic relaxation channels at 1.55 μm are more efficient in bundled SWNT than in MQW. Among them, nonradiative excitonic relaxation mechanisms are induced in semiconducting tubes like intraband decay or charge transfers by tunnel effect throughout metallic SWNT or example.[7] The 0.51 ps extracted recovery time of bundled SWNT is linked to the switching speed for SA, and is intrinsically close to the value obtained with Fe doped MQW grown by epitaxy (0.29 ps).[2] Let us also stress that more than 90% of recovery for transient absorption of SWNT is achieved in 2 ps. This absence of tail in absorption dynamics is of first importance as it allows clear absorption recovery of SA devices. These results demonstrating an ultrafast time recovery and total amplitude recovery make bundled SWNT promising candidates for 1.55 μm low-cost nanomaterials-based SA.

Other important parameters required for AOSR are the saturation amplitude and fluence values. Figure 3 reveals the excitation intensity dependence of the transient maximum NDT. These experimental data are adjusted by the semi-empirical absorption saturation law based on a two energy levels system:[17] $\Delta T/T_0=\exp[A/(1+SF/F)]-1$, where A is the absorbance of the sample, F is the excitation fluence, and SF the saturation fluence. SF corresponds to the input fluence

required for inducing switching phenomenon. First, we can notice here that the use of SWNT leads to a higher NDT than MQW with the same input pump fluence. As both nanomaterials provide relatively high value of NDT, a good contrast between the passing and blocking states of SA can be expected. Curve-fitting the experimental data with absorption saturation law, the extracted value of SF is 70 μJ cm^{-2} with A=0.19 for MQW. For SWNT, fits are not very sensitive to the saturation fluence as long as SF is above ~400 μJ cm^{-2}. Best fits correspond to SF=726 μJ cm^{-2} with A=2.04. In a telecom network, we are interested in optimizing the value of $\Delta T/T_0$ at a given fluence, which is a relevant key-parameter for AOSR.

Indeed, the quality of an optical data transmission channel is evaluated by the bit error rate parameter which is proportional to $Q^{-1}\exp(-Q^2/2)$, where $Q=(I_1-I_0)/(\sigma_1+\sigma_0)$ with $I_1(I_0)$ and $\sigma_1(\sigma_0)$ are the mean amplitude and standard deviation values of 1 and 0 optical symbols, respectively. The NDT is directly linked to the Q-factor since it contributes to increase the contrast (I_1-I_0) term. To improve $\Delta T/T_0$, one solution is to enhance the absorbance of SA based nanostructures.

In the case of SWNT, it consists in tuning the S1 absorption band of bundled SWNT films to the resonant excitation at 1.55 μm. Indeed, pump-probe spectroscopy with a wide continuum probe spectrum for micelles isolated SWNT in D_2O indicates that maximum values of $(\Delta T/T_0)$ perfectly match absorption spectra peaks of the sample.[18] Moreover the imaginary part of the third-order susceptibility (e.g., $|\mathrm{Im}\,\chi^{(3)}|$) determined by a Z-scan technique on bundled SWNT films shows a high enhancement under resonant excitation conditions for the lowest interband transition. $|\mathrm{Im}\,\chi^{(3)}|$ is linked to the variation of absorption and thus the maximum value of $(\Delta T/T_0)$.[19] One more technological step, like sorting by density gradient ultracentrifugation,[20] is needed to selectively tune absorption peaks of SWNT films near 1.55 μm.

In the case of MQW, another solution is based on the use of embedded MQW in a microcavity.[2] The idea is to enhance light-active zone interaction via the multiple reflections induced at the interfaces. As a consequence SF needed to induce switching phenomenon is reduced. For a well designed microcavity, destructive interferences of reflective waves can be exploited on device's surface so as to decrease T_0 level. Both solutions (enhancement of absorbance and reduction of SF and T_0) can be used for both nanostructures. Although they are not easy to implement and imply additional costs, they can be used to design high quality AOSR based SA.

In conclusion, transient transmission dynamics of HiPCO bundled SWNT deposited on glass substrate have been measured and compared to 40 periods Fe-doped InGaAs/InP MQW. Experimental data have been recorded in the same experimental run. Compared to MQW, bundled SWNT exhibit an intrinsically much faster recovery time, a relatively higher NDT as well as a few picosecond total recovery of the transient absorption.

Although NDT of SWNT has to be enhanced in order to match all AOSR telecom systems requirements, bundled SWNT confirm that they are good candidates for the future realization of low-cost and ultrafast SA for high-bit-rate AOSR in telecom networks.

This work (CASTEL project) is financially supported by the French Research National Agency (ANR-07-JCJC-0153-01) and is labeled by the "Media and Networks" cluster. Thanks to Julie Le Pouliquen for technical assistance and thanks to FOTON/ENSSAT for the using of the UV-Visible-IR spectrometer.

[1] H. M. Gibbs, A. C. Gossard, S. L. McCall, A. Passner, W. Wiegmann, and T. N. C. Venkatesan, Solid State Commun. **30**, 271 (1979).
[2] M. Gicquel-Guézo, S. Loualiche, J. Even, C. Labbé, O. Dehaese, A. Le Corre, H. Folliot, and Y. Pellan, Appl. Phys. Lett. **85**, 5926 (2004).
[3] M. Guézo, S. Loualiche, J. Even, A. Le Corre, H. Folliot, C. Labbé, O. Dehaese, and G. Dousselin, Appl. Phys. Lett. **82**, 1670 (2003).
[4] S. Iijima, Nature (London) **354**, 56 (1991).
[5] R. Saito, G. Dresselhaus, and M. S. Dresselhaus, *Physical Properties of Carbon Nanotubes* (Imperial College Press, London, 1998).
[6] V. Perebeinos, J. Tersoff, and P. Avouris, Phys. Rev. Lett. **92**, 257402 (2004).
[7] J.-S. Lauret, C. Voisin, G. Cassabois, C. Delalande, Ph. Roussignol, O. Jost, and L. Capes, Phys. Rev. Lett. **90**, 057404 (2003).
[8] Y. Kurashima, Y. Yokota, I. Miyamoto, H. Kataura, and Y. Sakakibara, Appl. Phys. Lett. **94**, 223102 (2009).
[9] E. J. R. Kelleher, J. C. Travers, Z. Sun, A. G. Rozhin, A. C. Ferrari, S. V. Popov, and J. R. Taylor, Appl. Phys. Lett. **95**, 111108 (2009).
[10] Y.-C. Chen, N. R. Raravikar, L. S. Schadler, P. M. Ajayan, Y.-P. Zhao, T.-M. Lu, G.-C. Wang, and X.-C. Zhang, Appl. Phys. Lett. **81**, 975 (2002).
[11] X. Xiao, J. Partridge, M. Taylor, and D. McCulloch, Phys. Status Solidi C **6**, 2179 (2009).
[12] D. Söderström, S. Marcinkevicius, S. Karlsson, and S. Lourdudoss, Appl. Phys. Lett. **70**, 3374 (1997).
[13] M. Guézo, S. Loualiche, J. Even, A. Le Corre, O. Dehaese, Y. Pellan, and A. Marceaux, J. Appl. Phys. **94**, 2355 (2003).
[14] O. J. Korovyanko, C.-X. Sheng, Z. V. Vardeny, A. B. Dalton, and R. H. Baughman, Phys. Rev. Lett. **92**, 017403 (2004).
[15] Y.-Z. Ma, L. Valkunas, S. M. Bachilo, and G. R. Fleming, J. Chem. Phys. B **109**, 15671 (2005).
[16] S. Schmitt-Rink, D. S. Chemla, and D. A. B. Miller, Phys. Rev. B **32**, 6601 (1985).
[17] D. S. Chemla, D. A. B. Miller, P. W. Smith, A. C. Gossard, and W. Wiegmann, IEEE J. Quantum Electron. **20**, 265 (1984).
[18] G. N. Ostojic, S. Zaric, J. Kono, V. C. Moore, R. H. Hauge, and R. E. Smalley, Phys. Rev. Lett. **94**, 097401 (2005).
[19] A. Maeda, S. Matsumoto, H. Kishida, T. Takenobu, Y. Iwasa, M. Shiraishi, M. Ata, and H. Okamoto, Phys. Rev. Lett. **94**, 047404 (2005).
[20] M. S. Arnold, A. A. Green, J. F. Hulvat, S. I. Stupp, and M. C. Hersam, Nat. Nanotechnol. **1**, 60 (2006).